Nat. Volatiles & Essent. Oils, 2021; 8(5): 3542 - 3562

NVEO
Natural Volatiles &
Essential Oils

Solar Panel Power Assisted Electric Vehicle Design And Development

[1]R.Sureshkumar, [2]S.Neelakrishnan , [3]Srinivasan P
[1,2,3] Department of Automobile Engineering
PSG College of Technology
rsk.auto@psgtech.ac.in

Abstract

This work intends to design and construct a solar-assisted electric car that is suited for Indian driving scenario, particularly in metropolitan locations, and then undertake research. It entails a study of driving conditions in Indian cities, as well as modelling and simulation for powertrain component size. After retrofitting solar panels and other associated devices, an examination of supplemental energy output under various situations was performed. Actual road testing was conducted to evaluate performance, energy savings, and increased range travelled per single charge. The traditional method of maximum power point monitoring is investigated, and a novel algorithm is used to shorten the time it takes to track the new power, allowing the output power to remain constant for longer.

Index Terms—Solar power, Battery pack, Power train, MPPT, MATLAB Simulation, Traction motor, Speed controller, Proteus simulation.

I. Introduction

1.1 Background and Motivation

Over the next several years, rising oil price, growing social concerns about climatic changes, and stringent rules concentrating on fuel/energy efficiency/CO2 emissions have the potential to trigger significant changes in the global car industry. Furthermore, the combined consequences of rising personal car usage and the worsening of urban air quality caused by fossil fuel-based transportation vehicles have prompted a move toward alternate modes of transportation and energy sources to power autos. For decades, electric powertrain has been studied as a potential replacement or supplement to the internal combustion engine. Electric vehicles (EVs) are the greenest alternative due to their zero local and maybe small greenhouse gas emissions. EVs generate no direct emissions, but the electricity they use comes from power generators emits variety of pollutants making severe ecological impacts. Nevertheless, due to poor performance, expensive costs, and short ranges, electric cars have failed to capture a major market share. EVs powered by renewable energy will minimise urban air pollution, rather than the point source of pollution caused by coal and fossil fuel.

1.2 Hybrid Electric Vehicle (Solar Assisted)

Solar energy is more plentiful, free, and equally distributed than other energy sources such as fossil fuels, uranium, wind, and water. Since the 1980s, researchers have been experimenting with photovoltaic systems for the propulsion of wheeled land transportation vehicles. However, due to substantial limits in solar technology, the creation of solar cars as a viable alternative to conventional fuel vehicles is presently not possible. There are now solar energy charging stations for EVs

accessible, however study indicates that incorporating solar panels inside EVs to replenish power generation and the utilization of EVs justifies further analysis [3,4].

1.3 Solar Power Assisted Hybrid Electric Vehicle

Because the surface area of solar panels on a car is constrained, it's critical to get the most out of them. Seasonal fluctuations also impact the quantity of available solar energy, limiting the amount of extra solar power generation available for EV propulsion [1-8]. Furthermore, these vehicles would require specialized energy management and control technologies. There are several interconnections between energy flows, propulsion system component sizing, vehicle size, performance, weight, and prices in these vehicles. After retrofitting flexible solar panels and other related equipment, an examination of supplemental energy output under various situations is conducted. Actual road testing was used to evaluate performance attributes, energy savings, and increased kms travelled per single battery charge. Solar energy not only enhances range and yet also decreases battery pack size, weight, and cost, with the primary target of decreasing fuel usage CO_2 emissions.

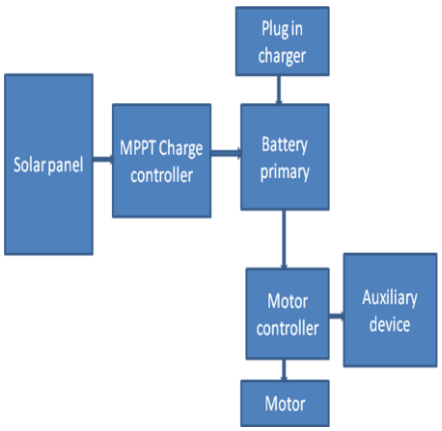

Fig.1 Generalized Schematic of a Solar Power Assisted Electric Vehicle

The use of public transportation in cities is increasing across the world. In the developing world, vehicle ridership is likely to continue to rise. Traditionally, fossil fuels have been used to power these vehicles. Poor urban air quality is exacerbated by air pollution caused by automobile emissions. EVs powered by renewable energy will minimise urban air pollution, point source pollution caused by non-renewable energy-based power plants, and overall reliance on fossil fuels. Solar power-assisted electric vehicles may use solar energy to generate electricity, lowering the requirement for non-renewable fuel-based power plants. In theory, solar-assisted electric vehicles might combine the benefits of both electric and solar vehicles by incorporating photovoltaic panels into an electric vehicle. As a result, solar-powered electric cars provide a potential answer to both energy conservation and environmental concerns. [5,6]

II. Selection of Solar Panel and Power Estimation

Solar Module

Solar cells, often known as photovoltaics, are electrical devices that convert sunlight directly into energy. Solar cells are linked in parallel or series to obtain the appropriate voltage and current. This configuration is known as a solar array or solar module.

Selection of Solar Panel

The solar panel is mainly selected based on their conversion efficiency and cost of the solar cell for that the conversion efficiency for the different material are tabulated below

Table 1 Solar Panel Efficiency Details

TYPES		EFFICIENCY (%)
Conventional panel	Mono crystalline silicon	(15 – 20)
	Poly crystalline silicon	(15 – 17)
Thin film panel	Amorphous silicon	(6 – 9)
	Cadmium telluride	(9 – 11)
	Copper indium based (gallium diselenide)	(10 – 12)

By comparing their conversion efficiencies and cost of different solar panels “wafer based mono crystalline photo voltaic module” is the more efficient near about 15-17% conversion efficiency and Rs.55Rs/watt. (Ref : USL PVT LTD). Also, its locally available in local city.

2.3 Power Estimation from the Solar Panel

The photo voltaic or solar cells are electronic devices that convert sunlight directly into electricity. To achieve required voltage and current the solar cells are connected in either parallel or series. This setup is called as solar array or solar module.

At clear sky solar irradiation in India 800 watts/m^2.

Conversion efficiency of our solar module is 18% (mono crystalline silicon).

But in Coimbatore (Southern Part of India) the average solar irradiation is 711 watts/m^2. This data is referred from NREL.

- Average irradiation is 711 watts/m^2
- Conversion efficiency of mono crystalline solar panel is 18%
- Power output per m^2 is 128

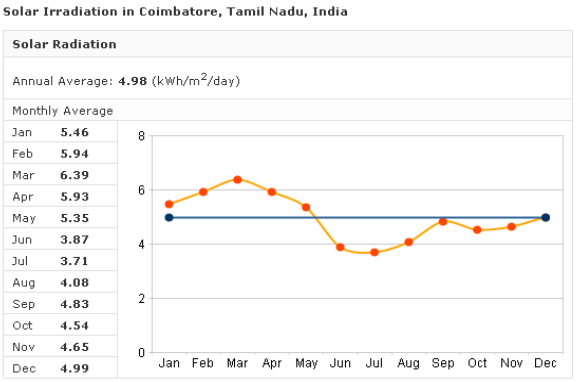

Fig 2 Solar Irradiation in Coimbatore

2.4 AREA AVAILABILITY FOR PANEL FIXING ON THE CAR:

Area of bonnet:

- Length - 700mm
- Breadth - 1095mm
- Area=L*B

$A1=0.76m^2$

Area of roof:

- Length - 1330mm
- Breadth - 1090mm
- Area=L*B

$A2=1.449\ m^2$

Area of goods place glass shield:

- Length - 700mm
- Breadth - 1095mm
- Area=L*B

$A3=0.76m^2$

Total area available:

A=A1+A2+A3

= 0.76+1.44+0.76

$A = 2.96\ m^2$

2.5 Estimation of Power Generation

- Area available is $2.96\ m^2$
- Power output per m^2 is =Average Irradiation(w/m^2) x conversion efficiency of panel

  P=7.11x 18

  P=128 W
- Power =area x watts/ m^2

= 2.96 x 128

= 379 Watts/ m^2

- Power generation/day commonly 8 hours per day is taken

  =379 x 8

  P=3.03kW/day

- Average power consumption/km distance travelling is 61 watts
- Additional distance can travel by this solar power is 49.68kms

3. Photovoltaic Cell

3.1 Single -Solar Cell Equivalent Circuit

Electrical model used to depict a solar cell. The following equation expresses voltage and current relation of the cell.

$$I = I_L - I_0\left(e^{\frac{q(V-IR_S)}{AkT}} - 1\right) - \frac{V-IR_S}{R_{SH}}$$

I and V - cell output current and voltage respectively

I_{0-} current at dark saturation conditions

q - electron's charge

A - diode quality factor

k - Boltzmann constant,

T - absolute temperature

R_S and R_{SH} - series and shunt resistance respectively.

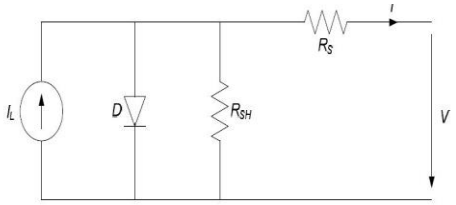

Fig . 3 Solar Cell Equivalent Circuit Model

PV panel comprised with several solar cells, interconnected in parallel/series connection. As a result, the PV panel's output current and voltage are sufficient to meet the grid's or equipment's requirements. Using the above-mentioned simplification, the output voltage and current responses from PV panel defined inequation (2). The ns and np and are cells in parallel and series connection, respectively [6]. A PV panel's output current-voltage characteristic is represented

$$I \approx n_p I_L - n_p I_O\left(e^{\frac{q(V-IR_S)}{AkTn_S}} - 1\right) \quad \text{....(2)}$$

Effect of solar radiation variation

$$Iph = [Isc + Ki(T - 298)]\frac{\beta}{1000}$$

Cell variation temperature

$$Is(T) = Is\left(\frac{T}{Tnom}\right)^3 e^{\left[\left(\frac{T}{Tnom}-1\right)\frac{Eg}{N,Vt}\right]}$$

3.2 MMPT, Open Circuit Voltage and Short Circuit Current

The V_{OC} (open circuit) voltage and I_{SC} (short circuit) current are two significant aspects of the current-voltage characteristic that must be mentioned. The electricity generated is 0 at both places. At instance cell's output current is zero, i.e. I=0, and the shunt resistance RSH is ignored, VOC can be

estimated from (1). Equation is used to express it (3). As indicated in equation, the short circuit current I_{SC} is current when V = 0 and approximately equivalent to the photon light produced current I_L (4).

$$V_{OC} = \frac{AkT}{q} \ln \left(\frac{l_L}{I_0} + 1 \right)$$

$$I_{sc} \approx I_L$$

The solar cell generates the most power at a position on the IV curve where the product VI is highest. This point is referred to as the tracking with maximum power point

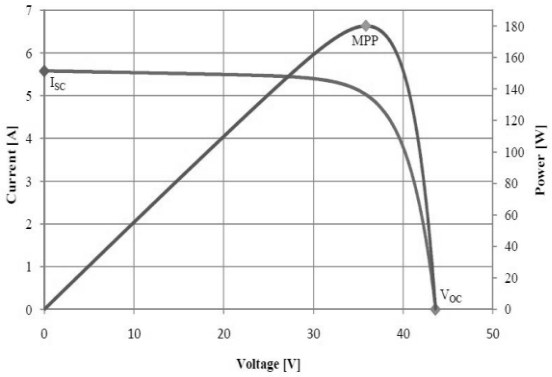

Fig 3 Solar Panel Characteristic Curves

3.3 Fill Factor (FF)

The FF may be calculated with the help of MPP I and V, VMPP and I_{MPP},V_{OC} and ISC equation governed by

$$FF = \frac{V_{MPP} I_{MPP}}{V_{OC} I_{SC}}$$

It is a frequently used metric for assessing the overall quality of solar cells. the ratio of actual maximum power to power- theoretical maximum (ISCVOC), which isn't achievable. This is caused by parasitic series and shunt resistances in analogous circuit The maximum FF rating for diose will be around 0.7.

4. Power Electronic- Boost Converter

4.1 Boost Converter

A boost converter belongs to the switch-mode DC-DC converter family. By switching mode sequences, the DC voltage can be either step up/down as per driving operations. Energy stored by

passive components inductors or capacitors will perform the conversion by connecting in series and shunt arm. Conversion efficiency varies s from 75 to 98% with loses dissipated due to heat.

The design equations can be formulated and anlysed from the following equations

$$V_o = \frac{1}{T}\int_0^{T_{ON}} V_{in}dt = \frac{V_{in}}{T}[t]_0^{T_{ON}}$$

$$\Rightarrow V_o = \frac{V_{in}}{T}T_{ON} = k * V_{in}$$

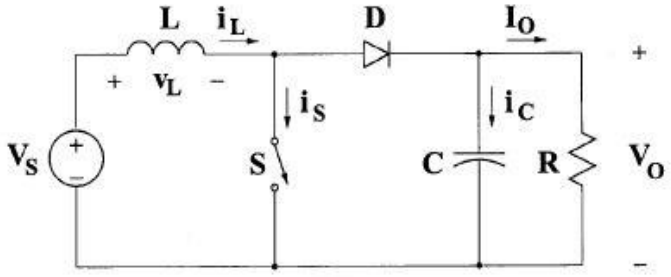

Fig 4 Circuit diagram of boost converter

The boost converter in which current inductor increases by turning on switch S, and the diode D is turned off. When the switch S is switched off, the inductor's stored energy is freed to the RC circuit via diode. Output RC circuit receives a discontinuous current. As a result, in comparison to buck-derived converters, a bigger filter capacitor is required to reduce ripple output voltage. When diode D, turned-off, filter element capacitor must send the DC output to the load.

4.2 INDUCTOR AND CAPACITOR DESIGN

The external components must be precisely estimated for the circuit to operate properly. The voltage across the inductor is increased when the switch is turned on.

$$V_L = L\frac{di}{dt} = L\frac{I_{LKP}}{t_{on}}$$

and the current expressed by

$$I_{on} = \left[\frac{V_{in} - V_{sat}}{L}\right]t_{on}$$

When the switch off, the voltage at inductor is expressed by

$$V_L = L\frac{di}{dt} = L[\frac{I_{Lmin} - I_{LPK}}{t_{off}}]$$

and the current represented by

$$I_{Loff} = I_{Lpk} - \left[\frac{V_{out} + V_F - V_{in}}{L}\right] t_{off}$$

forward voltage ($V_{F)}$ drop is output rectifier voltage and saturation voltage (V_{sat}) of the output .

The operating frequency for boost converter selected by

$$t_{on} + t_{off} = \frac{1}{f} = 50\mu s \qquad (11)$$

The inductor value can be chosen as

$$L = \frac{V_{in} * k}{I_{ripple} * F_s}$$

The capacitor value is chosen by

$$C = \frac{I_o * k}{V_{ripple} * F_s}$$

where V_{in} is the expressed input voltage

I_o - output current

k - duty cycle

F_s - switching frequency

4.3 Power Point Tracking Maximum (MPPT)

MPPT processes are essential in PV panels because the MPP of a panel fluctuates due to irradiance and temperature variations, with the necessitating employment of MPPT implementation to get maximum power in solar array.

Many approaches for locating the MPP being developed and articulated during few in recent years. These approaches differ in various ways, including the number of sensors required. In addition, cost, complexity, price, convergence speed, effectiveness range, accurate tracking when irradiation and/or variations in temperature, the hardware required for execution, and their popularity. There is a comprehensive study of 19 distinct MPPT algorithms available.

The incremental conductance (InCond) and Perturb-Observe algorithms are the most popular of the strategies described. These strategies have the benefit of being simple to use, but they also have disadvantages, as will be demonstrated later. Artificial neural networks (ANN), Fuzzy logic control are opted by researchers to switch off voltage and current control.

5 . Perturb and Observe Algorithm

Because of its simplicity, the P&O techniques with the most integrated with MPPT algorithm. The flow chart for the P&O approach is shown in Figure 4.1. The current power is computed after each perturbation operation and compared to the prior value to ascertain the power change.

The most often used MPPT algorithm is the P&O approach. If P>0, the procedure proceeds in the same perturbation direction. Otherwise, the process will reverse the direction of perturbation.

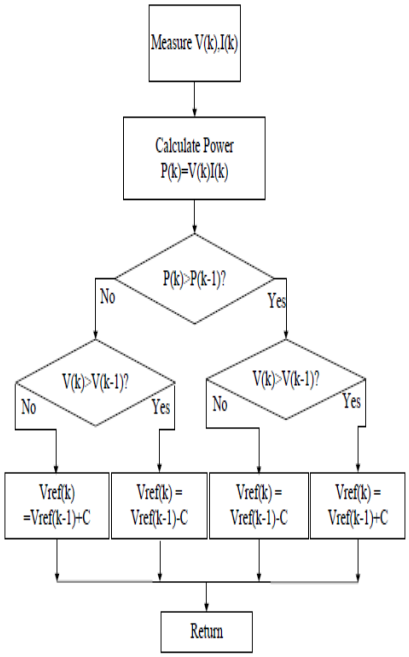

Fig 5. Flow Chart of P&O algorithm

Magnitude of voltage references increase predicts quickly MPP in both P&O and InCond systems. These approaches consist of two major flaws. The first is the most important when irradiation varies shortly, they can easily lose track of the MPP. They follow MPP extremely well when there are step changes since the shift is immediate and the curve does not alter. During irradiation changes along an incline, however, curve on algorithms discretized with radiation changes., perturbation

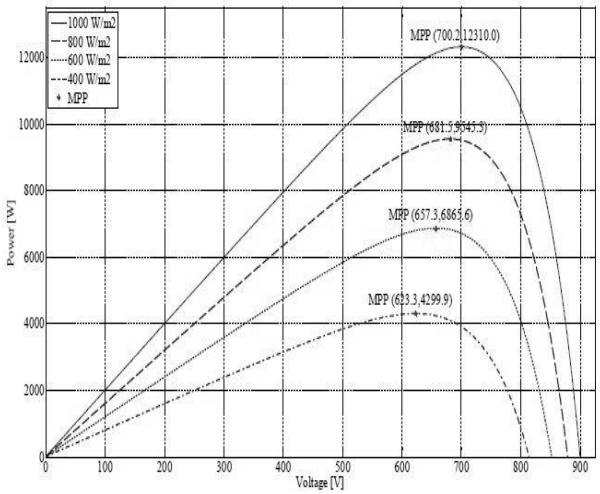

Fig 6 Power-Voltage Curve Irradiation Profiles

Fluctuations in current and voltage near the MPP in the steady state are another flaw of both approaches. This is because control discretized, and the current and voltage are fluctuating about the MPP rather of being constant. The magnitude of the oscillations is determined by the reference voltage's rate of change. The higher it is, the larger the oscillations' amplitude.

6. Simulation Results and Discussion

6.1 Overview

Simulink is a piece of software that allows you to model, simulate, and analyse dynamic systems. It allows you to ask a question about a system and model it. Simulink makes it simple to create new models or alter old ones to match your needs. Simulink allows you to simulate linear and nonlinear models in continuous systems, sampling. Various elements of a system can sampled for multi variate systems. Simulink allows go beyond idealized with linearized models and investigate added realistic nonlinear models that incorporate with vehicle running resistances.

6.2 Simulink Model of Solar Panel

Simpower system block set and math operation block set are used to model PV cells in the MATLAB Simulink environment. The PV equations are presented in the Simulink model below.

$$I \approx n_p I_L - n_p I_O \left(e^{\frac{q(V - IR_S)}{AkTn_s}} - 1 \right)$$

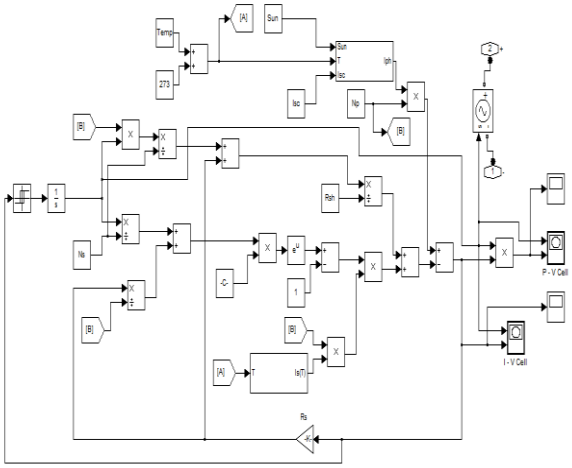

Fig 7 Simulink Model of PV equations

Effect of Solar Radiation Variation

$$Iph = [Isc + Ki(T - 298)]\frac{\beta}{1000}$$

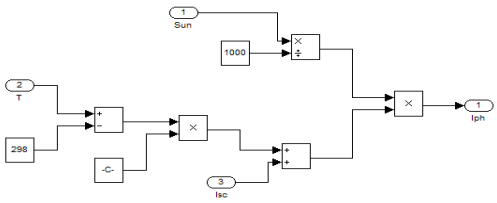

Fig 8 Effect of Solar Radiation Variation

Effect of varying cell temperature

$$Is(T) = Is\left(\frac{T}{Tnom}\right)^3 e^{\left[\left(\frac{T}{Tnom} - 1\right)\frac{Eg}{N,Vt}\right]}$$

7. Simulation Results of Solar Panel

Monocrystalline solar panels are employed in this project. Each panel is made up of 36 cells that are linked in a series. The data for the solar panel simulation was derived from the data sheet provided by the panel manufacturer. With varied irradiation and temperature, the output voltage, current, and power from a single panel are simulated.

Input parameters taken for simulation.

Effect of solar irradiation variation

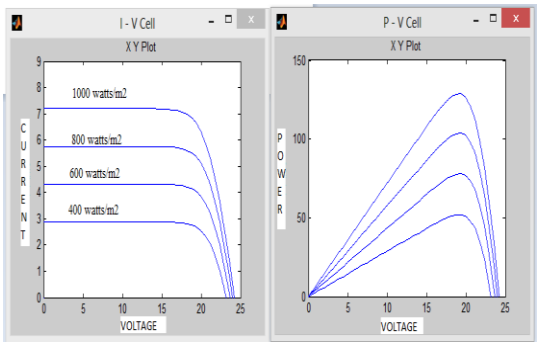

Fig 9 Graph for Effect of Solar Irradiation Variation

The effect of irradiation variation is depicted above fig. Where output power is varies with respect to irradiation if the irradiation is increasing the power output also increases similarly if it decreases then output also will get decrease.

Also, one more important thing the maximum output power we can get at peak point only. So, to get more effective power generation should track the maximum power point. This tracking is done by MPPT technique.

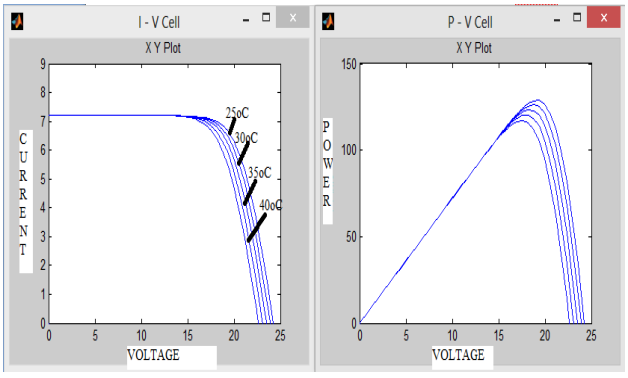

Fig 10 Effect of Varying Cell Temperature

The output power fluctuates as the temperature changes, as seen in the diagram above. According to the graph, as temperature elevates, by decrease in the voltage, and as the cell temperature reduces, the output voltage.

7.1 Modeling of MPPT Algorithm

Solar power systems are typically fitted with the feature of MPPT to surge the availability of solar energy and hence the system's total efficiency. The mathematical model for the method given above was created using the Simpower system block set from Simulink.

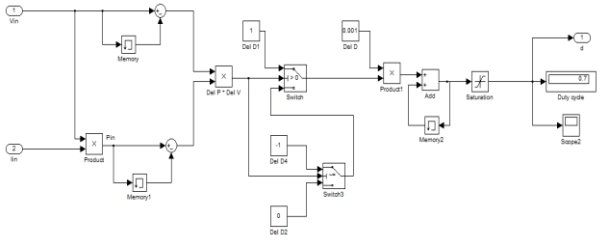

Fig 11 Simulink model- P& O Method Algorithm

The P&O technique is a dynamic MPP finding approach that is widely used in solar power systems. It's usually done by looking at the output voltage and power before and after the perturbation and identifying the MPP from the P–V curve.

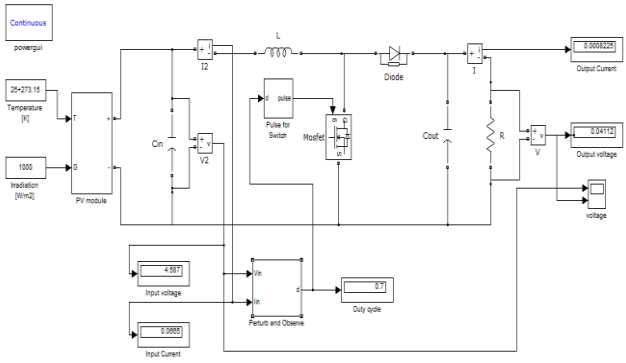

Fig 12 Simulink model of P&O method

7.2 MPPT Simulation Component Calculations

Vi = 34.2 Volts; Vo = 50 Volts;
Ii = 12.88 Amps; Io= 8.8 Amps;
Power =440 Watts;
ΔVc = 5% of Vo ΔI = 3% of Io

$$\Delta Vc = \frac{50}{100} * 5 = 2.5$$

$$\Delta I = \frac{8.8}{100} * 3 = 0.264$$

$$K = 1 - \frac{Vi}{Vo} = 1 - \frac{34.2}{50} = 0.316$$

Clock Frequency = 25KHZ

$$T = \frac{1}{F} = \frac{1}{25000} = 0.00004 \text{ Sec}$$

$$L = \frac{Vi * K}{f * \Delta I} = \frac{34.2 * 0.316}{25000 * 0.264} = 1.6374 \text{mH}$$

$C = \frac{Io * K}{f * \Delta Vc} = \frac{8.8 * 0.316}{25000 * 2.5}$ = 44.49e-6 F

$R = \frac{Vo}{Io} = \frac{50}{8.8}$ = 5.68 Ohm

Fig 12 Real Time Testing of Solar Panel

Fig 13 voltage and Current Measurement

Fig 14 Irradiation measurement using flux meter

Fig 15 Temperature Measurement

8. Analysis and Selection of Traction Motor

DC series motors are commonly used in traction applications where high torque/speed ratios are required [9]. As variable speed drives, DC motors are still the most widely used machinery. Modeling DC machinery is much easier than modelling AC ones. Controlling DC motors has become much

easier because to advancements in design of choppers and rectifiers. DC series motor machines and PMDC (permanent magnet machines) are the most often utilised DC machines for power electronic DC drives. Changing polarity terminal voltage of a DC motor to change its speed is a relatively typical application.

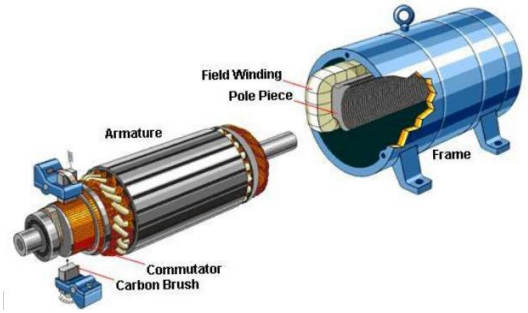

Fig 16 DC motor Construction

The motor will be chosen based on the amount of power necessary to propel the vehicle. This is determined by the vehicle's weight and the required max speed. Vehicle dynamics are used to calculate the amount of power necessary to propel the vehicle.

Wheel Speed

Motor operating speed assumed at 1500 rpm to calculate vehicle velocity.

$$Nw = \frac{\mathrm{Nm}}{\mathrm{GB} * \mathrm{FD}}$$

$$Nw = \frac{1500}{.9 * 4.38}$$

N_w= 350 rpm

Velocity

From the wheel speed velocity of the car is calculated

$$V = \frac{\pi * \mathrm{D} * \mathrm{Nw} * 60}{1000}$$

$$V = \frac{\pi * .508 * 380 * 60}{1000}$$

V=36.36km/hr

Total Resistance

Total resistance expressed by

Rt=Rolling Resistance + Aerodynamic Resistance

Rt= Crr*W+1/2*ρ*A*V^{2*}Cd

M=(Veh-550;battery-180;panel+motor-100+280)1060kg ;

V=36.36km/hr;

Dw=.508m

Rt=0.015*9.8*1060+0.5*1.22*1.6*(36.36*.277)^2* 0.35

Rt=192.02N

Power Required

$$p = \frac{\mathrm{Rt} * \mathrm{V}}{3600 * \eta}$$

$$P = \frac{192.02 * 36.36}{3600 * .88}$$

P=2.2kW≈3Hp

Torque @ 750 RPM

$$T = \frac{2.2 * 60000}{2 * \pi * 750}$$

$$T = \frac{\mathrm{P} * 60000}{2 * \pi * \mathrm{Nm}}$$

T=28.02Nm

Tractive Effort

$$TE = \frac{\mathrm{Tm} * \mathrm{GB} * \mathrm{FD} * \eta}{\mathrm{r}} TE = \frac{28.02 * 3.58 * 4.38 * .95}{.254}$$

TE=1643 N

Acceleration

F=ma

F=TE-Rt

TE=1643N

Rt=192N

m=1060kg

a=1.36m/s^2 **@36.36km/hr**

t=7.4sec

Distance Travel/Charge

Battery pack=48V*150Ah

=7200

Constant load power consumption P=2.2kW

Battery power supply in hours @ constant load=3.27hrs

Distance can travel

D=V x hours; =36.36 x 3.27

D = 118 km.

Power Consumption /km

Power P=7200/118

P=61W/km

Maruti 800 specifications

- Top speed of that vehicle is 120km/hr so total resistance offered by vehicle is high.
- Rolling resistance=155
- Aerodynamic resistance=403.2

- Total resistance Rt=558
- Power required

$$p = \frac{\mathrm{Rt} * \mathrm{V}}{3600 * \eta}$$

P=21.14kw≈29bhp

Here gradient & Acc resistance is not added.

From the above calculations the power required to propel the vehicle is 3hp but here chosen the 5hp motor has a traction motor.

Selected Motor Specifications

Type -DC Series motor
Voltage - 48 Volt
Armature current- 75 Amps
Output power - 3.7KWp
Speed - 1500rpm

Speed Controller Design

An electric motor's accelerator pedal is normally mechanically connected variable resistances, which converts position as voltage signal provided as voltage regulation. The pedal signal conditioning to remove rheostat disturbances and smooth rapid shifts speed increases and slowdowns is therefore a primary purpose for this control. This conditioned signal is then used by the speed control for its second function, which is to generate the switching. This is attained by PWM modulation control.

DC motor speed control -Developed

The functions of producing PWM switching signal processing the power electronic chopper. Several analogue modules and their individual components are replaced by a single CPU. The physical sizes and manufacturing prices of the control can therefore be decreased while its dependability is enhanced. The suggested speed control is depicted in Fig. 1 as a block diagram. The DSPIC30F2010 microcontroller is utilised here, and it has eight A/D converters.

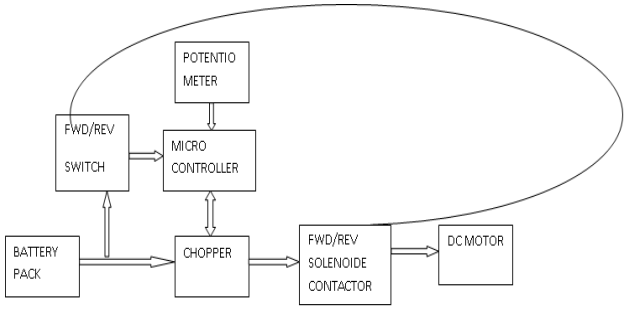

Fig 17 Block Diagram for Speed Controller

9. Hardware Development of Speed Controller

The first step in the hardware kit development is selection of power rating for each component. These power ratings are based on selected motor ratings.

List of components used controller are

1. Two quadrant choppers
2. Microcontroller
3. Solenoid switch contactors
4. Linear pot meter (throttle control)
5. Switch driver
6. Fwd/Rev switch

Here DSPIC30F2010 microcontroller is used to generate PWM signal. These signals are weak, so it's given to gate terminal of IGBT switch through driver circuit to amplify the generated signals. This microcontroller is having two inputs one is FWD/REV control switch and another one is linear type pot meter for acceleration control.

The connections are shown in block diagram.

Microcontroller and Driver circuit

Two quadrant IGBT module

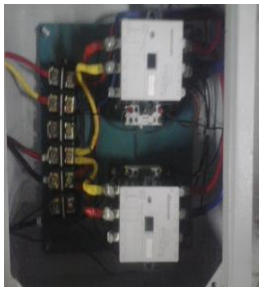

Solenoid Contactors

Linear pot meter

Testing of speed controller

Fig.17 Traction Drive Testing

10. Analysis and Selection of Battery Pack

Traction EVs batteries are differs from conventional batteries. The parameters like C-rate, specific energy density, power density, cost, battery management systems (BMS). From lead acid to lithium ion to lithium air are evolution of batteries are utilized for electric vehicles.

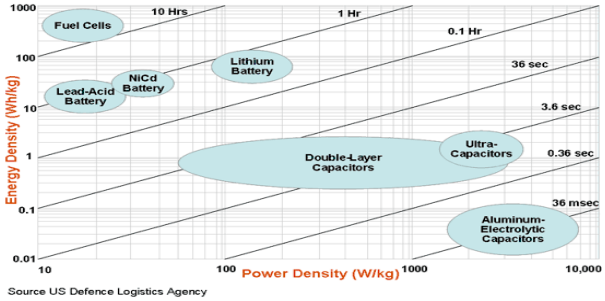

Fig 18. Ragone Plot

Lead-acid batteries have long been the most common option for electric vehicles. High-capacity lead-acid batteries may be created and are economical, safe, and dependable. They have a recycling system in place. Low specific energy density and power density are limitations however based on the cost and availability constrained the lead acid battery utilized for this work.

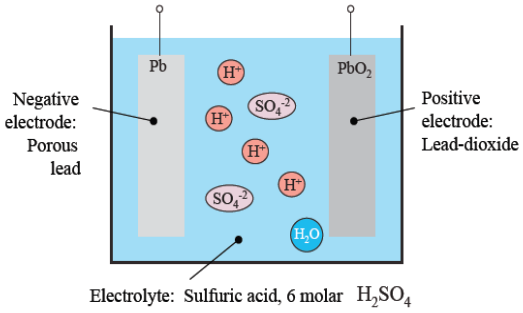

Fig. 19 Lead Acid Battery Cell Operation

Battery cell operates when a cell discharge, when the energy is supplied from the battery to the electric motor to develop propulsion power, and a cell charge operation. Reduction/oxidation (REDOX) are the charging and discharging reactions happens inside the cell compartment.

10.1 Power Rating of Traction Battery

Here four 12V deep cycle discharge traction battery is chosen and each having 150Ah power rating.

Fig. 20 Battery Stacking

7.2kw power can store by this battery. It can supply the power up to 118 km per charge with 60 watts per kilometer continues power consumptions i.e. 2.2 kW continues load.
While plug in charging we can charge 50 volt and 10 amps rating.

10.2 Assembly of SPAEV

To develop this SPAEV chosen the maruti 800 vehicle and replaced IC engine by electric motor,

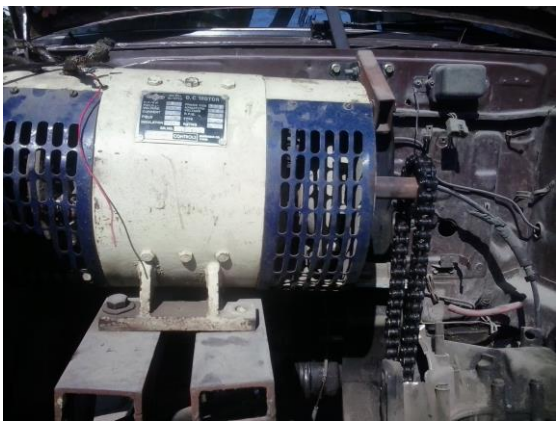

Fig 21 Electric Motor Assembly

The panels are mounted on bonnet, roof and rear dickey door, and battery pack is placed on rear goods place.

Fig 22 Solar Panel Assembly

The main reason for selecting this vehicle is to suit the driving needs of Indian riders also less weight.

11 Conclusion

The area of the car's bonnet and roof space, different types of solar panels, various methods of MPPT algorithm, battery selection by comparing its basic properties, different types of motors that can be used for traction by comparing their speed torque characteristics, and easy speed control methods are all examined. In addition, the conversion efficiency, area of availability in the automobile, and battery power rating are all factors in choosing the right solar panel. The mono crystalline conventional 440-watt solar panel was used in this case.

A suitable MPPT algorithm is chosen and implemented based on numerous analyses. Based on the foregoing inference, a MATLAB/Simulink model is created, and the results are assessed and generated. The P&O algorithm was chosen and a hardware kit was constructed for it.

The best power rating traction motor is chosen based on the vehicle's power requirements, strong starting torque, and an accurate and simple speed control approach. Here, a 5hp DC series motor was used, and a speed controller was also constructed for it. The armature voltage control approach is employed for the speed controller. The maximum current rated by the speed controller is 200 amps. To save money, just two quadrant choppers were employed for speed control, and forward and reverse operations were handled by two external contactors.

The battery pack is chosen based on the motor ratings and the distance to be travelled. Because the motor's rated voltage and current are 48 volts and 75 amps, a 48 volt and 150 amps lead acid battery pack was used. Lead acid batteries are inexpensive and widely accessible.

To construct this, SPAEV picked a Maruti 800 car and replaced the IC engine with an electric motor; panels are put on the bonnet, roof, and rear dickey door; and the battery pack is in the back goods compartment. The key reason for choosing this vehicle is because it meets the demands of Indian riders while still being light.

REFERENCES

1. Hussein, K.H., Murta,I., Hoshino,T., Osakada,M.,“Maximum photovoltaic power tracking: an algorithm for rapidly changing atmospheric conditions”, IEEE Proceedings of Generation,
2. E. Koutroulis, et. Al, “Development of a Microcontroller-based photovoltaic maximum power tracking control system”, IEEE Trans. On power Electron, VOl.16, No. 1, PP.46-54, 2001,
3. A.Jiang et. Al.,”Maximum Power Tracking for Photovoltaic Power Systems,” Tamkang Journal of Science and Engineering, Vol. 8, No. 2, pp. 147-153, 2005.
4. Environment”, Proce. of IEEE International Conference on Clean Electrical Power, ICCEP 2007, Capri, Italy.
5. Jesus Leyva-Ramos, Member, IEEE, and Jorge Alberto Morales-Saldana," A design criteria for the current gain in Current Programmed Regulators", IEEE Transactions on industrial electronics, Vol. 45, No. 4, August 1998.
6. K.H. Hussein, I. Muta, T. Hoshino, M. Osakada, "Maximum photovoltaic power tracking: an algorithm for rapidly changing atmospheric conditions", IEE Proc.-Gener. Trans. Distrib., Vol. 142,No. 1, January 1995.
7. Y.V. Bocharnikov, A.M. Tobias, C. Roberts, S. Hillmansen, C.J. Goodman, Optimal driving strategy for traction energy saving on DC suburban railways, Electric Power Applications, IET 1 (September (5)) (2007) 675–682.
8. F. Ruelland, K. Al-Haddad, Reducing Subway’s Energy, in: Proceedings Electrical Power Conference, IEEE Canada, 25–26 October, 2007, pp. 261–267.
9. Castagnet T, Nicolai J. Digital control for brush DC motor. IEEE Tran Ind Appl 1994;30(4):883–8.
10. OngChee-Mun. Dynamic Simulation of Electric Machinery UsingMATLAB/S IMULINK. New Jersey: Prentice Hall; 1998.
11. subcircuit-models of power devices. IEEE Proceedings of CIEP, International Power Electronics Congress; 1998. p. 158–63.
12. Goody RW. MicroSim PSPICE for Windows. New Jersey: Prentice Hall; 1998.
13. Krause PC, Wasynczuk O, Sudhoff SD. Analysis of Electric Machinery. New York: IEEE Press; 1995.

14. Mohan N, Underland TM, Robins WP. Power Electronics Converters, Applications and Design.New York: John Wiley and Sons; 1995.
.Sen PC, MacDonald ML. Thyristorized DC drives with regenerative braking and speed reversal.IEEE Trans IECI 1978;25(4):347–54.
15. Argueta OJ. Desarrollo e Implementaci_on de un Control de Velocidad e Motores de CD en Serie, MSc Thesis, Centro de Investigaci_on y Estudios Avanzados del IPN, Unidad Guadalajara, 1999.
16. DeWolf FT. Measurement of inductance of DC machines, IEEE Trans. Power Apparatus and Systems 1979; PAS-98(5):1636–44. MATLAB, 1999. Reference Manual.
17. Muhammad HR. Power electronics circuits, devices and applications. Prentice Hall Inc. 1993.
18. Pagiela, Energy storage system with ultracaps on board of railway vehicles, in: European Conference on Power Electronics and Applications, 2–5 September, 2007, pp. 1–10.
19. M. Brenna, F. Foiadelli, E. Tironi, D. Zaninelli, Ultracapacitors application for energy saving in subway transportation systems, in: Proceedings International Conference on Clean Electrical Power, 21–23 May, 2007, pp. 69–73.
20. F. Foiadelli, M.C. Roscia, D. Zaninelli, Optimization of storage devices for regenerative braking energy in subway systems, in: IEEE PES General Meeting, Montreal, Canada, 18–22 June, 2006.
21. H.-J. Chuang, C.-S. Chen, C.-H. Lin, C.-H. Hsieh, C.-Y. Ho, Design of optimal coasting speed for saving social cost in Mass Rapid. Transit systems, in: Proceedings 3rd International Conference on Electric Utility Deregulation and Restructuring and Power Technologies, 6–9 April, 2008, pp. 2833–2839.